

Gaussian Process Model for Collision Dynamics of Complex Molecules

Jie Cui and Roman V. Krems

Department of Chemistry, University of British Columbia, Vancouver, B.C., V6T 1Z1, Canada

(Dated: December 7, 2024)

We show that a Gaussian Process model can be combined with a small number of scattering calculations to provide an accurate multi-dimensional dependence of scattering observables on the experimentally controllable parameters (such as the collision energy, temperature or external fields) as well as the potential energy surface parameters. This can be used for solving the inverse scattering problem, the prediction of collision properties of a specific molecular system based on the information for another molecule, the efficient calculation of thermally averaged observables and for reducing the error of the molecular dynamics calculations by averaging over the potential energy surface variations. We show that, trained by a combination of classical and quantum dynamics calculations, the model provides an accurate description of the scattering cross sections, even near scattering resonances. In this case, the classical calculations stabilize the model against uncertainties arising from wildly varying correlations of resonantly enhanced quantum results.

The outcome of a molecular collision in a thermal gas is a complicated function of many parameters: the collision energy, the internal energy of molecules, the details of the intermolecular potential energy surface (PES) and the relative orientation of the colliding species. Providing a mapping between these parameters and the scattering observables is a very complex task, paramount to solving the inverse scattering problem [1, 2] and critical for the interpretation as well as the physical interpolation or extrapolation of experimental data. Knowing the dependence of observables on the PES is also critical for assessing the accuracy of the scattering calculations and averaging the dynamical results over PES variations to reduce the uncertainties [3, 4]. For simple systems, this mapping can be provided by a series of classical [5] or quantum scattering [6] calculations on a grid of internal energy, collision energy, relative angular momentum and/or the PES parameters [3, 4]. This approach quickly becomes impossible as the complexity of molecules increases. Even for simple molecules, the role of the potential is often examined by scaling the PES by a single multiplicative factor, which does not change the topology of the PES [7]. For polyatomic molecules and to explore the effect of the PES topology, it is necessary to examine the observables as functions of all (usually many) parameters determining the PES. For example, a realistic PES for the interaction of benzene with structureless atoms must be parametrized by ≥ 8 constants [8, 9] and it is clearly impossible to carry out dynamical calculations on an 8-dimensional grid of the PES parameters.

An alternative approach could be to develop an analytical function of the scattering observables on the underlying parameters by fitting the calculated values, for example, with spline functions or regressions [10]. However, any such fit would require many data points as a function of every parameter to infer the proper analytical dependence. This becomes impossible as the complexity of molecules increases and when the collision dynamics is affected by resonances leading to dramatic varia-

tions of observables, extremely sensitive to PES [11, 12]. Here, we propose an approach combining a small number of scattering calculations with a Gaussian Process (GP) model [13, 14]. Widely used in engineering technologies [15, 16], the GP model learns from correlations between data points and provides a non-parametric dependence of observables on the underlying parameters. We show that, trained by the classical trajectory (CT) and/or quantum scattering calculations, the GP model provides an efficient and accurate model of molecular collisions, giving the simultaneous dependence of the scattering observables on all of the underlying parameters, without the need to fit any data by analytical functions. A combination of the CT and quantum calculations provides an accurate GP model of the scattering cross sections, even near scattering resonances. In this case, the CT calculations stabilize the model against uncertainties arising from wildly varying correlations of resonantly enhanced quantum results.

To illustrate the accuracy and efficiency of the model we consider the scattering cross sections and the formation of long-lived collision complexes of benzene molecules placed in a cold environment of rare gas (Rg = He – Xe) atoms. Collisions of complex organic molecules with Rg atoms at low temperatures have recently received much attention due to the buffer gas cooling experiments [17–19]. In these experiments, molecules are thermalized by momentum-transfer collisions with the buffer gas atoms, while the formation of long-lived collision complexes leads to clustering and impedes the thermalization. We show that the GP model can be used to obtain the dependence of the collision lifetimes on the rotational temperature and the collision energy of the molecule, the mass of the Rg atom as well as on the details of the PES for atom - molecule interactions.

We consider a scattering observable \mathcal{O} as a function of q parameters described by vector \mathbf{x} . The components of the vector $\mathbf{x} = (x_1, x_2, \dots, x_q)^\top$ can be the collision energy, the internal energy and/or the parameters rep-

representing the PES. We assume that \mathcal{O} is known from a classical or quantum dynamics computation at a small number of \mathbf{x} values. Our first goal is to construct an efficient model that, given a finite set of $\mathcal{O}(\mathbf{x})$, produces a global dependence of the scattering observable on \mathbf{x} . If the same observable is measured as a function of some parameters x_i – e.g., the collision energy – we show that the model can be adjusted to produce the global dependence of \mathcal{O} on \mathbf{x} that reproduces the experimental data, even if the dynamical calculation method is inaccurate.

We assume that the scattering observable of interest at any point \mathbf{x} in this multi-dimensional parameter space is a realization of a Gaussian process $F(\cdot)$, characterized by a mean function $\mu(\cdot)$, constant variance σ^2 and correlation function $R(\cdot, \cdot)$. For any fixed \mathbf{x} , $F(\mathbf{x})$ is a value of a function randomly drawn from a family of functions Gaussian-distributed around $\mu(\cdot)$. Consequently, the multiple outputs $F(\mathbf{x})$ and $F(\mathbf{x}')$ produced at two different points \mathbf{x} and \mathbf{x}' are random variables that jointly follow a multivariate normal distribution completely defined by $\mu(\cdot)$, σ^2 , and $R(\cdot, \cdot)$ [20, 21]. We assume the following form for the correlation function [22–25]:

$$R(\mathbf{x}, \mathbf{x}') = \exp \left\{ - \sum_{i=1}^q \omega_i |x_i - x'_i|^p \right\}. \quad (1)$$

and write

$$F(\mathbf{x}) = \sum_{j=1}^k h_j(\mathbf{x}) \beta_j + Z(\mathbf{x}) = \mathbf{h}(\mathbf{x})^\top \boldsymbol{\beta} + Z(\mathbf{x}), \quad (2)$$

where $\mathbf{h} = (h_1(\mathbf{x}), \dots, h_k(\mathbf{x}))^\top$ is a vector of k regression functions [26], $\boldsymbol{\beta} = (\beta_1, \beta_2, \dots, \beta_k)^\top$ is a vector of unknown coefficients, and $Z(\cdot)$ is a Gaussian random function with zero mean. The problem is thus reduced to finding $\boldsymbol{\beta}$, p and $\boldsymbol{\Omega} = (\omega_1, \omega_2, \dots, \omega_q)^\top$.

We spread n input vectors $\mathbf{x}_1, \dots, \mathbf{x}_n$ evenly throughout a region of interest and compute the desired observable \mathcal{O} at each \mathbf{x}_i with a classical or quantum dynamics method. The outputs of a GP at these points $\mathbf{Y}^n = (F(\mathbf{x}_1), F(\mathbf{x}_2), \dots, F(\mathbf{x}_n))^\top$ follow a multivariate normal (MVN) distribution

$$\mathbf{Y}^n \sim \text{MVN}(\mathbf{H}\boldsymbol{\beta}, \sigma^2 \mathbf{A}) \quad (3)$$

with the mean vector $\mathbf{H}\boldsymbol{\beta}$ and the covariance matrix $\sigma^2 \mathbf{A}$. Here, \mathbf{H} is a $n \times k$ design matrix with i th row filled with the k regressors $h_1(\mathbf{x}_i), h_2(\mathbf{x}_i), \dots, h_k(\mathbf{x}_i)$ at site \mathbf{x}_i , and \mathbf{A} is a $n \times n$ matrix defined as

$$\mathbf{A} = \begin{pmatrix} 1 & R(x_1, x_2) & \cdots & R(x_1, x_n) \\ R(x_2, x_1) & 1 & & \vdots \\ \vdots & & \ddots & \\ R(x_n, x_1) & \cdots & & 1 \end{pmatrix} \quad (4)$$

Given $\boldsymbol{\Omega}$, the maximum likelihood estimators (MLE) of $\boldsymbol{\beta}$ and σ^2 have closed-form solutions [13]:

$$\hat{\boldsymbol{\beta}}(\boldsymbol{\Omega}) = (\mathbf{H}^\top \mathbf{A}^{-1} \mathbf{H})^{-1} \mathbf{H}^\top \mathbf{A}^{-1} \mathbf{Y}^n \quad (5)$$

$$\hat{\sigma}^2(\boldsymbol{\Omega}) = \frac{1}{n} (\mathbf{Y}^n - \mathbf{H}\boldsymbol{\beta}) \mathbf{A}^{-1} (\mathbf{Y}^n - \mathbf{H}\boldsymbol{\beta})^\top \quad (6)$$

To find the MLE of $\boldsymbol{\Omega}$, we fix p and maximize the log-likelihood function

$$\log \mathcal{L}(\boldsymbol{\Omega} | \mathbf{Y}^n) = -\frac{1}{2} [n \log \hat{\sigma}^2 + \log(\det(\mathbf{A})) + n] \quad (7)$$

numerically by an iterative computation of the determinant $|\mathbf{A}|$ and the matrix inverse \mathbf{A}^{-1} .

The goal is to make a prediction of the scattering observable at an arbitrary $\mathbf{x} = \mathbf{x}_0$. Because the values $Y_0 = F(\mathbf{x}_0)$ at \mathbf{x}_0 and the outputs at training sites are jointly distributed, the conditional distribution of possible values $Y_0 = F(\mathbf{x}_0)$ given the values \mathbf{Y}^n is a normal distribution with the conditional mean and variance given by

$$m(\mathbf{x}_0)^* = \mathbf{h}(\mathbf{x}_0)^\top \boldsymbol{\beta} + \mathbf{A}_0^\top \mathbf{A}^{-1} (\mathbf{Y}^n - \mathbf{H}\boldsymbol{\beta}) \quad (8)$$

$$\sigma^{*2}(\mathbf{x}_0) = \sigma^2 (1 - \mathbf{A}_0^\top \mathbf{A}^{-1} \mathbf{A}_0), \quad (9)$$

where $\mathbf{A}_0 = (R(\mathbf{x}_0, \mathbf{x}_1), R(\mathbf{x}_0, \mathbf{x}_2), \dots, R(\mathbf{x}_0, \mathbf{x}_n))^\top$ is specified by the now known correlation function $R(\cdot, \hat{\boldsymbol{\Omega}})$. Eq. (8) provides the GP model prediction for the value of the scattering observable at \mathbf{x}_0

To illustrate the applicability and accuracy of the GP model, we first compute the collision lifetimes of benzene molecules with Rg atoms [27, 28]. This is a critical parameter that determines the probability of benzene molecules to collect atoms into molecule-centered clusters by three-body recombination. We use the CT method described in Ref. [27]. As shown in Ref. [8], the C_6H_6 - Rg interaction potentials can be expressed as a sum over terms describing the interaction of Rg with the C-C and C-H bond fragments, characterized by 8 parameters. We first fix the PES parameters to describe the C_6H_6 - Ar system and focus on the dependence of the lifetimes on two parameters: the collision energy E and the rotational temperature T_r . Figure 1 (upper panels) shows the results of the CT calculations illustrating that the collision lifetime exhibits an inverse correlation with the collision energy, while no apparent correlation with the rotational temperature. Figure 1 (c) shows the global surface of the lifetime as a function of E and T_r obtained from the GP model with $h_1 = 1, h_{i>1} = 0$ and p set to 1.95. To quantify the prediction accuracy of the GP model, we calculate the errors $\varepsilon_E = \sqrt{\frac{1}{n} \sum_{i=1}^n (y_i - \hat{y}_i)^2}$ and $\varepsilon_S = \varepsilon_E / (y_{\max} - y_{\min})$. For the model with only 20 scattering calculations used as training points, $\varepsilon_E = 9.36$ ps and $\varepsilon_S = 7.93$ %. If the number of the scattering calculations is increased to 50, the errors decrease to $\varepsilon_E = 5.17$ ps and $\varepsilon_S = 4.38$ %.

Scattering data interpolation. The scattering calculations presented in the upper panels of Figure 1 cannot be interpreted to assume any simple functional form. In addition, the vastly different gradients of the T_r and E dependence may make the conclusions based on calculations at fixed values of one of the parameters misleading.

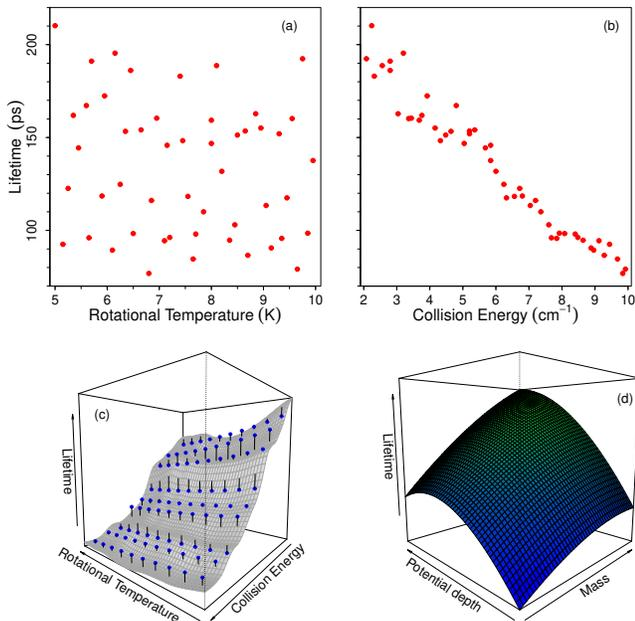


FIG. 1. (a) and (b): The lifetime dependence on the rotational temperature and collision energy for $\text{C}_6\text{H}_6 - \text{Ar}$ collisions. (c): The surface produced by the GP model. The lines connect the values (circles) computed from the classical trajectories with the values predicted by the GP model. (d): The surface produced by the GP model for $\text{C}_6\text{H}_6 - \text{Rg}$ collision lifetimes vs the atomic mass and the PES depth for $T_r = 4 \text{ K}$ and $E = 4 \text{ cm}^{-1}$.

In contrast, the surface plot in Figure 1(c) clearly illustrates that the collision lifetimes decrease monotonically with both T_r and E . The effect of the rotational temperature is much weaker especially when $E > 5 \text{ cm}^{-1}$ and there is no strong two-way interaction between T_r and E . The GP model surface can be used to evaluate thermally averaged collision lifetimes by integrating the E -dependence at given T_r .

The GP model can be extended to multiple collision systems for the predictions of the collision properties of a specific molecule based on the known collision properties of another molecule. To illustrate this, we consider the lifetimes of the long-lived complexes formed by benzene in collisions with Rg atoms He – Xe. As the collision system is changed from $\text{C}_6\text{H}_6 - \text{He}$ to $\text{C}_6\text{H}_6 - \text{Xe}$, there are two varying factors that determine the change of the collision dynamics: the reduced mass and the PES. These factors must be correlated but the correlations cannot be clearly determined from the scattering calculations for different systems because the dependence of the scattering observable on these two parameters is very different.

As before, we use the GP model $F(\mathbf{x}) = \beta + Z(\mathbf{x})$, with \mathbf{x} now representing the atomic mass μ_A and the interaction strength D_e at the global minimum of the

atom - molecule PES obtained by scaling the Ar - C_6H_6 PES. We fix $T_r = 4 \text{ K}$ and the collision energy $E = 4 \text{ cm}^{-1}$, and compute the collision lifetimes at 40 randomly chosen points in the interval of μ_A and D_e [$4\text{g/mol}, 130\text{g/mol}$] \times [$80\text{cm}^{-1}, 520\text{cm}^{-1}$], which covers all of the Rg - C_6H_6 systems. These 40 calculation points are then used to train the GP model to produce the surface plot shown in Figure 1 (d). The error ε_S of the surface is 5.09 %. The plot reveals that increasing both μ_A and D_e enhances the collision lifetimes and that the reduced-mass dependence of the collision lifetimes is very weak compared to the dependence on the interaction strength.

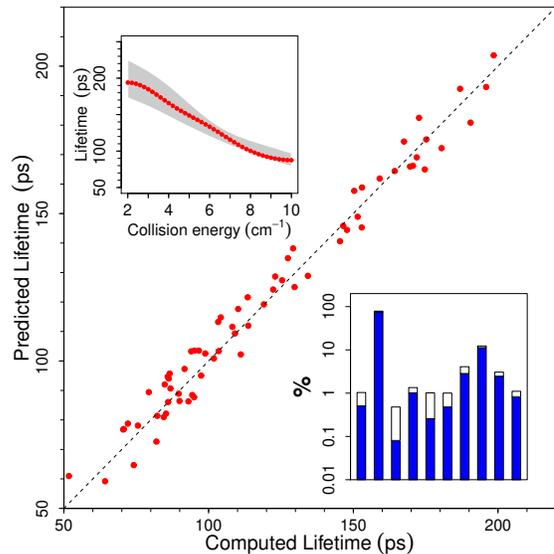


FIG. 2. Accuracy of the GP model with variable PES parameters for the prediction of the collision lifetimes. The scatter plot compares the predicted values with the computed values. The error of the GP model is the deviation of the points from the diagonal line. Left inset: Energy dependence of the collision lifetime for Ar - C_6H_6 with the error interval obtained by varying *all* the individual PES parameters by $\pm 3 \%$. Right inset: Relative effect of the variation of T_r , E and the PES parameters on the collision lifetimes. The filled area of the bars shows the uncorrelated contribution of the corresponding variable and the open area – the effect that depends on one or more other variables.

Multi-dimensional model. The GP model can be exploited to explore the role of the individual PES parameters on the scattering observables. To illustrate this, we now consider that the vector \mathbf{x} contains 8 parameters giving the analytical form of the Rg - C_6H_6 PES [8], in addition to E and T_r . We calculate the lifetimes of the Rg - C_6H_6 collisions at 200 randomly selected points in this parameter space and use these points to train the GP model. To illustrate the prediction accuracy of the GP model thus produced, we plot in Figure 2 the predicted magnitudes of the lifetimes for another set of 70

randomly selected points vs the quantities produced by the CT calculations. The plot corresponds to the model error $\epsilon = 4\%$.

The 10-parameter GP model contains a wealth of information on the dependence $\mathcal{O}(\mathbf{x})$. For example, one can perform a sensitivity analysis by using the functional analysis of variance decomposition [29–31] to determine, which of the PES parameters have the strongest impact on the observable (right inset of Figure 2). Of the 8 PES parameters, the location of the potential well due to the interactions of Rg with the C-C bonds for the parallel approach [8] is the most important factor determining the collision lifetime. The model can also be used to compute the uncertainties due to *global* variation of the PES. Figure 2 (left inset) shows the interval of the lifetimes obtained by the simultaneous $\pm 3\%$ variation of all 8 PES parameters.

Fitting experimental data. The GP model can be extended to fit the experimental observations by varying the PES, with the fit absorbing both the measurement error and the error of the dynamical calculations. To illustrate this, consider an ensemble of randomly generated pseudo-experimental data (circles in Figure 3) and assume that the molecular dynamics calculation is affected by unknown errors. The off-set of the data from the dashed diagonal line represents the inaccuracy of the molecular dynamics calculations. The scatter of the data points represents the measurement error. We first partition the vector \mathbf{x} into two parts: \mathbf{x}_E containing the parameters that can be varied in experiments (such as the collision energy or temperature) and \mathbf{x}_P containing all the other variables including the PES parameters. We then write the model for the experimental data as [32]

$$E(\mathbf{x}_E|\mathbf{x}_P) = \rho F(\mathbf{x}_E, \mathbf{x}_P) + G(\mathbf{x}_E) + \epsilon, \quad (10)$$

where $F(\cdot)$ and $G(\cdot)$ are independent Gaussian random functions, with $G(\cdot)$ characterizing the inaccuracy of the scattering calculations, and ϵ is a Gaussian-distributed variable characterizing the measurement errors. The calculations are performed in three steps. First, the scattering calculations are used to train the GP model $F(\cdot)$ of the *scattering calculation data*. In the second step, the experimental and calculated data are used together to train the model $G(\cdot)$ in Eq. (10), using the parameters of $F(\cdot)$ from the first step averaged over possible values of \mathbf{x}_P and treating ρ and ϵ as variable parameters. This fixes the models $F(\cdot)$ and $G(\cdot)$ as well as ρ and ϵ . Given these, Eq. (10) can be used to find the best-fitting PES parameters by using Markov chain Monte Carlo methods [33]. The inset of Figure 3 illustrates the accuracy of the GP model (10) without further optimization of the parameters \mathbf{x}_P . The scatter plot of the inset has the error $\epsilon_S = 6.3\%$.

Eq. (10) can also be used to model time-consuming quantum scattering calculations with the help of much more efficient classical dynamics calculations. To illus-

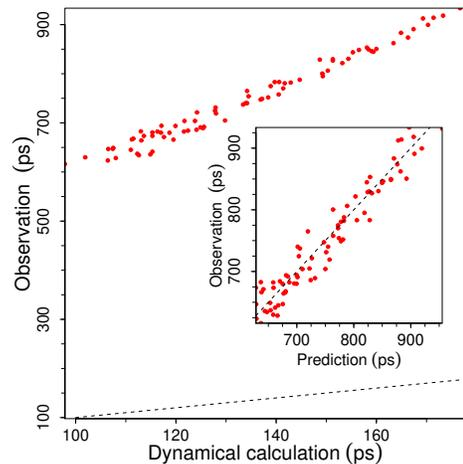


FIG. 3. Randomly generated pseudo-observation data (red circles) vs the results obtained from the CT calculations. The off-set of the data points from the dashed line represents the inherent inaccuracy of the scattering calculations. Inset: Accuracy of the GP model (10).

trate this, we consider the cross sections for rotationally inelastic $C_6H_6 - He$ collisions [9] shown in Figure 4. Sixty randomly chosen quantum results are used to train the model (10) with ϵ set to zero and $G(\cdot)$ modeling the inaccuracy of the CT calculations. Figure 4 shows that the model provides an accurate energy dependence of the cross sections, even near scattering resonances. The scattering resonances make the direct model (2) unstable, as shown in Figure 4 (inset). The CT calculations in a two-function model (10) stabilize the model, removing the errors arising from the resonant variation of the quantum results.

In summary, we have shown that a Gaussian Process model combined with a small number of scattering calculations can be used to obtain an accurate multi-dimensional dependence of the scattering observables on the experimentally controllable parameters and the PES parameters. In the absence of the experimental data, the GP model can be trained by a limited set of scattering calculations to provide a multi-parameter fit of the calculation results. This can be used to integrate the results over some of the parameters in order to evaluate efficiently thermally averaged quantities or to average the scattering calculations for complex molecules over variations of the PES parameters, thereby minimizing the uncertainties due to PES inaccuracies. If experimental data are available, they can be reproduced by a combination of two independent GP models: one trained to model the scattering calculations and one to model the uncertainty of the scattering calculation method. The same model can be used to connect classical and quantum dynamics calculations, allowing one to use classical calculations to interpolate quantum results. The model

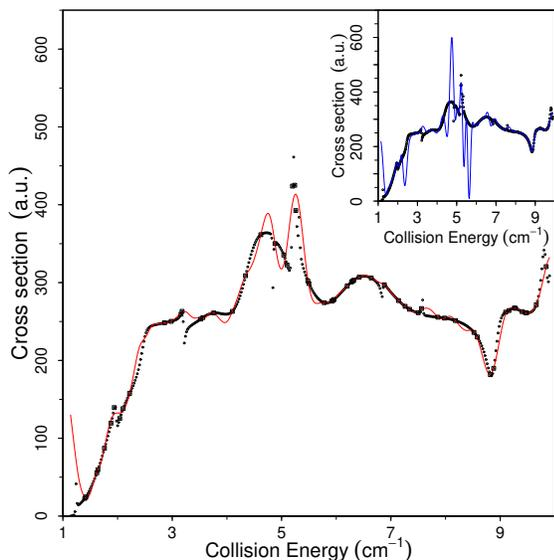


FIG. 4. GP model (solid curve) of quantum scattering cross sections (squares and circles) for C_6H_6 - He collisions with CT calculations (not shown) serving as an intermediate model. The 60 squares are the quantum results used to train the models. The inset shows the GP model (solid curve) trained by the quantum results without CT calculations.

described here is expected to find a wide range of applications, from fitting the interaction potentials by solving the inverse scattering problem, to analyzing the dependence of scattering observations on external parameters, to calibrating the accuracy of the scattering calculation methods.

We thank Zhiying Li for allowing us to use her codes for the classical and quantum dynamics calculations. This work is supported by NSERC of Canada.

[1] S. Shi and H. Rabitz, *Comp. Phys. Rep.* **10**, 3 (1989).
 [2] R. Baer and R. Kosloff, *J. Phys. Chem.* **99**, 2534 (1995).
 [3] M. D. Frye and J. M. Hutson, *Phys. Rev. A* **89**, 052705 (2014).
 [4] M. L. González-Martínez and J. M. Hutson, *Phys. Rev. Lett.* **111**, 203004 (2013).
 [5] R. B. Bernstein (ed.), *Atom-Molecule Collision Theory*, Plenum, New York (1979).
 [6] N. F. Mott and H. S. W. Massey, *The theory of atomic collisions*, Oxford University Press (1965).
 [7] Y. V. Suleimanov, T. V. Tscherbul, and R. V. Krems, *J. Chem. Phys.* **137**, 024103 (2012).
 [8] F. Pirani, M. Albertí, A. Castro, M. Moix Teixidor, and

D Cappelletti, *Chem. Phys. Lett.* **394**, 37 (2004).
 [9] Z. Li, R. V. Krems and E. J. Heller, *J. Chem. Phys.* **141**, 104317 (2014).
 [10] J. O. Ramsay and B. W. Silverman, *Functional data analysis*, Springer (2005).
 [11] K. Liu, R. T. Skodje and D. E. Manolopoulos, *Phys. Chem. Chem. Comm.* **5**, 27 (2002).
 [12] C. Chin, R. Grimm, P. Julienne, and E. Tiesinga, *Rev. Mod. Phys.* **82**, 1225 (2010).
 [13] J. Sacks, W. J. Welch, T. J. Mitchell, and H. P. Wynn, *Stat. Sci.* **4**, 409 (1989).
 [14] C. E. Rasmussen, *Gaussian processes in machine learning*, In *Advanced lectures on machine learning*, Springer (2004).
 [15] D. Higdon, M. Kennedy, J. C. Cavendish, J. A. Cafeo, and R. D. Ryne, *SIAM J. Sci. Comput.* **26**, 448 (2004).
 [16] D. Higdon, J. Gattiker, B. Williams, and M. Rightley, *J. Am. Stat. Assoc.* **103**, 482 (2008).
 [17] D. Patterson, E. Tsikata, and J. M. Doyle, *Phys. Chem. Chem. Phys.* **12**, 9736 (2010).
 [18] D. Patterson and J. M. Doyle, *Phys. Chem. Chem. Phys.*, in press (2015).
 [19] D. Patterson, M. Schnell, and J. M. Doyle, *Nature* **497**, 475 (2013).
 [20] R. J. Adler, *The geometry of random fields*, SIAM (2010).
 [21] H. Cramér and M. R. Leadbetter, *Stationary and related stochastic processes: Sample function properties and their applications*, Courier Corporation (2013).
 [22] T. Mitchell, M. Morris, and D. Ylvisaker, *Stoch. Proc. Appl.* **35**, 109 (1990).
 [23] N. A. Cressie, *Statistics for spatial data*, Wiley, New York (1993).
 [24] M. L. Stein, *Interpolation of spatial data: some theory for kriging*, Springer (1999).
 [25] M. Abt, *Scand. J. Stat.* **26**, 563 (1999).
 [26] The regression functions can be chosen to follow a specific parametric dependence of the calculated data in order to make the GP model more efficient. If no such dependence is known or can be determined, the regression functions can simply be chosen as $h_1 = 1$ and $h_{i>1} = 0$, reducing the first term in Eq. (2) to a constant β .
 [27] Z. Li and E. J. Heller, *J. Chem. Phys.* **136**, 054306 (2012).
 [28] J. Cui, Z. Li and R. V. Krems, *J. Chem. Phys.* **141**, 164315 (2014).
 [29] G. Pujol, *Sensitivity: Sensitivity analysis. R package version 1.4-0* (2008).
 [30] A. Saltelli, M. Ratto, T. Andres, F. Campolongo, J. Cariboni, D. Gatelli, M. Saisana, and S. Tarantola, *Global sensitivity analysis: the primer*, Wiley (2008).
 [31] O. Roustant, D. Ginsbourger, and Y. Deville, *J. Stat. Softw.* **51**, 54 (2012).
 [32] M. Kennedy and A. O'Hagan, *J. Roy. Statist. Soc. Ser. B* **63**, 425 (2001).
 [33] W. K. Hastings, *Biometrika* **57**, 97 (1970).